A NOVEL METHOD FOR ADAPTIVE ENHANCEMENT AND UNSUPERVISED SEGMENTATION OF MRI BRAIN IMAGE

Jing-Hao XUE, Wilfried PHILIPS, Aleksandra PIZURICA, and Ignace LEMAHIEU *

Department of Telecommunications and Information Processing, Ghent University
*Department of Electronics and Information Systems, Ghent University
St.-Pietersnieuwstraat 41, B9000 Gent, Belgium. E-mail: Wilfried.Philips@telin.rug.ac.be

ABSTRACT

This paper describes a novel global-to-local method for the adaptive enhancement and unsupervised segmentation of brain tissues in MRI (Magnetic Resonance Imaging) images. Three brain tissues are of interest: CSF (CerebroSpinal Fluid), GM (Gray Matter), WM (White Matter). Firstly, we de-noise the image using wavelet thresholding, and segment the image with minimum error thresholding. Both the thresholdings are global-wise. Subsequently, we combine locally adaptive weighted median and weighted average filters with FCM (Fuzzy C-Means) clustering to achieve a local-wise segmentation. The performance of the proposed method is quantitatively validated by four indices with respect to a MRI brain phantom.

1. INTRODUCTION

Segmentation of brain tissues in MRI images, plays an indispensable role in three-dimensional (3-D) volume visualization, quantitative morphometric analysis, and structure-function mapping for both scientific and clinical investigations. For instance, in order to construct the mapping between EEG (ElectroEncephaloGram) and MRI, an anatomic head model is necessary with segments of CSF, GM, WM, the skull and the scalp because of the significantly different conductivities of these tissues. In this paper, we deal with the segmentation of CSF, GM and WM in MRI images.

Numerous methods have been reported in this area [1, 2]. Niessen et al. [2] grouped roughly these methods into three main directions: classification methods, region based methods and boundary based methods. Just as pointed out in [2], the methods in the first two directions are limited by the difficulties due to intensity inhomogeneities, partial volume effects and susceptibility artifacts, while those in the last direction suffer from spurious edges. Furthermore, all the methods are also degraded by noise perturbations in low contrast and low SNR (Signal-to-Noise Ratio) images, e.g., the images used in EEG/MRI mapping with thin slices and a short measuring time.

In this context, we propose a global-to-local method to achieve an adaptive enhancement and unsupervised segmentation of CSF, GM and WM. Our method is a hybrid of an unsupervised classification method (Fuzzy C-Means clustering) and a region based method (minimum error thresholding). Partial volume effects are taken into account by calculating fuzzy membership degree of a pixel to these three brain tissues. In order to remove the noise and artifacts, a global filter based on wavelet thresholding, and segmentation-based locally adaptive weighted median and weighted average filters are also embedded into our method.

2. OUTLINE OF PROPOSED METHOD

The outline of our method is described as follows.

First we de-noise the image using wavelet thresholding. Second we segment the image with minimum error thresholding. Both the thresholdings are global-wise. Third we classify the pixels into three brain tissues through an FCM clustering, using the global thresholding result to initialize the parameters of FCM. The feature space is constructed by intensity pairs (intensity, average intensity) of the pixels in the MRI image. Fourth, we de-noise the image again with locally adaptive weighted median and weighted average filters; the elements of filtering templates are decided by the clustering result and weighted by the fuzzy membership degrees. Finally we employ the FCM clustering once more to achieve a local-wise segmentation.

3. DE-NOISING WITH WAVELET THRESHOLDING

Wavelet transforms have an ability of locating frequency contributions in the spatial domain. This ability facilitates the wide use of wavelet thresholding for image de-noising [3, 4] by suppressing those coefficients that originate from noise.

The common procedure of wavelet based de-noising is the following: 1) Compute the wavelet decomposition of the noisy image; 2) Modify the wavelet coefficients: the coefficients supposed to be dominated by noise are usually replaced by zero, other coefficients are either kept unchanged or reduced; 3) Reconstruct the de-noised image from the modified coefficients.

Donoho and Johnstone [3] classified the coefficient having its absolute value below a "universal threshold" into the set of coefficients dominated by noise. The universal threshold is derived as: $t_u = \hat{\sigma} \cdot \sqrt{2\log(n)}$, where n is the number of wavelet coefficients, and $\hat{\sigma} = MAD/0.6745$ is the estimates of the noise standard deviation. MAD denotes the Median Absolute Deviation of the wavelet coefficients in the finest resolution level. The wavelet coefficients $w_{j,k}$ above the universal threshold are updated by soft thresholding: $sgn(w_{j,k})(|w_{j,k} - t_u|)$.

The magnitude of MRI images is generally Rician distributed, as the acquired complex MRI data is known to be corrupted by Gaussian white noise [5]. The Rician distribution approaches to a Gaussian distribution when SNR is high.

In this step, our goal is to improve the SNR thus to approximate more precisely the Rician distribution with Gaussian distribution by a fast and effective de-noising. Gaussian distribution is more easy to be processed, whatever in mathematics or in engineering application, especially it is the base of the following minimum er-

ror thresholding. Higher SNR will also give rise to a better segmentation in further FCM clustering, considering more compact and well-separated intensities of brain tissues. Meanwhile, wavelet thresholding with universal threshold doesn't considered the spatial intra-scale or inter-scale correlation. It brings blurring more or less into the reconstructed image. Therefore, a tradeoff has to be made here between the efficiency and the effectiveness.

We employed an one level decomposition with Daubechies wavelets $db4$. From the experiments, we found there is not much difference in using different wavelets. An MRI image simulated from a normal brain phantom [6] with 9% noise level and 40% intensity inhomogeneity is shown in Fig. 1(a), along with its denoising result in Fig. 1(b).

4. MINIMUM ERROR THRESHOLDING

In our global-to-local method, we use FCM clustering to achieve spatial adaptive segmentation. As an unsupervised clustering method, FCM has its performance, particularly the validity and speed of convergence, being dependent on the initialization of its parameters, e.g., the centers (prototypes) of clusters, the membership degrees of each pixel to different clusters. The random initialization leads quite possibly the FCM to converge to a local minimum or a saddle point of its objective function. To decrease such a possibility, a reliable initialization is required.

Practically, due to a great diversity of MRI images from different subjects and imaging settings, and due to an aim of reducing the human interactivity in favor of a less labor-intensive and fast segmentation, no prior knowledge of the parameters of FCM is available straightforwardly. However, these parameters can be estimated through an initial segmentation which constructs automatically the training set of classified pixels in the original image.

In order to generate a fast and reliable estimator of FCM's parameters, intensity-based thresholding is used in our work. Intensity-based thresholding is the most old, simple and widely used segmentation algorithm. Since the Rician distributed MRI data can be better approximated by Gaussian distribution after the wavelet de-noising, we choose minimum error thresholding proposed by Kittler and Illingworth [7] and based on Gaussian distributions of objects and background intensities.

Although this method is originally proposed for a binarization, it can be extended to segment three clusters of the CSF, GM and WM. Suppose a threshold pair $\mathbf{t} = (t_1, t_2)$, $1 < t_1 < t_2 < 256$ for an 8 bits T1-weighted MRI image where the black background with zero intensity is always ignored in processing, we use this pair to classify all the pixels having an intensity f into a cluster c: c is CSF (if $f < t_1$), GM (if $t_1 \leq f < t_2$) or WM (if $f \geq t_2$).

Considering a probability $p(f)$ of the intensity f, a priori probability $P(c|\mathbf{t})$ of the cluster c, and a conditional probability $p(f|c, \mathbf{t})$ of f given that f is classified into c under $\mathbf{t}$, one criterion of an optimal classification is to maximize a sum $\sum_{f\in[1,256)}[p(f)\cdot P(c|\mathbf{t})p(f|c,\mathbf{t})]$. Suppose that we approximate the $p(f)$ by the intensity histogram $h(f)$, and approximate the $p(f|c, \mathbf{t})$ by three Gaussian distributions $N(\mu_{c,\mathbf{t}}, \sigma^2_{c,\mathbf{t}})$ for c as being CSF, GM or WM respectively, then the mentioned criterion can be viewed as a measure of fitting between the observed intensity distribution and the Gaussian approximation. We seek the pair $\mathbf{t}$ corresponding to the maximum fitting. An alternative criterion can be obtained by minimizing $\sum_{f\in[1,256)}[-2p(f)\cdot\log(P(c|\mathbf{t})p(f|c,\mathbf{t}))]$ so as to simplify the computation. Consequently, the objective function can be rewritten as

$$J(\mathbf{t}) = \sum_c [P(c|\mathbf{t})\log\sigma_{c,\mathbf{t}} \; - \; P(c|\mathbf{t})\log P(c|\mathbf{t})] \; , \qquad (1)$$

where $P(c|\mathbf{t})$, $\sigma_{c,\mathbf{t}}$ can be estimated from the histogram $h(f)$ [7].

The global threshold pair $\mathbf{t}$ can be found by minimizing the $J(\mathbf{t})$ in equation (1). The intensity-based thresholding result of Fig. 1(a) is shown in Fig. 1(c); it will be used to initialize the parameters of the following FCM clustering.

5. LOCAL-WISE SEGMENTATION WITH FCM

FCM is an iterative, unsupervised clustering algorithm, initially developed by Dunn and later generalized by Bezdek [8]. FCM has been applied widely to MRI segmentation, and regarded as one of the most promising methods [1].

Consider a dataset $X = \{\mathbf{x}_k\}_{k=1}^n \subset R^q$ where q is the dimension of the desired feature space, $\mathbf{x}_k$ denotes the feature vector of k-th data sample; and a set of fuzzy subsets $\{F_i\}_{i=1}^C$ with its corresponding crisp versions $\{H_i\}_{i=1}^C$. FCM partitions X into F_i with a mapping $u_i : X \mapsto [0, 1]$. $u_{ik} \triangleq u_i(\mathbf{x}_k)$ designates the membership degree of a data sample $\mathbf{x}_k$ in the F_i, and $\sum_{i=1}^C u_{ik} = 1, \forall\, k$.

The optimal partition is accessed via minimizing approximately the sum of intra-cluster squared errors as

$$J_{FCM}(U, V : X) = \sum_{i=1}^{C}\sum_{k=1}^{n}(u_{ik})^m(\|\mathbf{x}_k - \mathbf{v}_i\|)^2, \qquad (2)$$

where matrix $U = [u_{ik}]_{C\times n}$, while set $V = \{\mathbf{v}_i\}_{i=1}^C$, $\mathbf{v}_i \in R^q$ is the prototype of i-th cluster F_i. $m \geq 1$ is a weighting exponent which determines the degree of fuzziness of FCM. $\|\mathbf{x}_k - \mathbf{v}_i\|$ is an inner product induced norm on R^q to measure the distance from $\mathbf{x}_k$ to $\mathbf{v}_i$; we use the Euclidean norm and set $m = 2$.

In order to bring the locally spatial information from the image into the FCM clustering, we compute a two-dimensional feature vector of (intensity, locally average intensity) for each data sample, i.e., $\mathbf{x}_k = (f_k, \bar{f}_k)' \in R^2$ where f_k is the intensity of k-th data sample, and $\bar{f}_k$ the corresponding local average. We choose the simple 8-connectivity for local averaging. Generally the pixels inside of a homogeneous region are located closer to the main diagonal than the edge pixels. Hence we choose such a feature space.

In our case three subsets $\{F_i\}_{i=1}^3$ are defined respectively for CSF, GM and WM, so $C = 3$. The two features characterize themselves in the same range $[1, 256)$, so no normalization is used. We implement FCM to segment brain tissues as follows.

Step 1: Initialize U using the minimum error thresholding result as: if the k-th data sample (corresponding to $\mathbf{x}_k$) is segmented into H_i, $u_{ik} = 1$; otherwise $u_{ik} = 0$. Initialize V as

$$\mathbf{v}_i = \sum_{k=1}^{n}(u_{ik})^m\mathbf{x}_k \;/\; \sum_{k=1}^{n}(u_{ik})^m \; , \; \forall\; i \; . \qquad (3)$$

and $\mathbf{v}_i^{(0)} = \mathbf{v}_i$.

Step 2: Update U as: $\forall\; \mathbf{x}_k$, count the number (β) of prototypes which satisfy $\|\mathbf{x}_k - \mathbf{v}_i\| = 0$, Υ denotes a set of these prototypes; if $\beta \neq 0$, then $\forall\; \mathbf{v}_i \in \Upsilon$, $u_{ik} = 1/\beta$; otherwise

$$u_{ik} = \Big[\; \sum_{j=1}^{C}(\|\mathbf{x}_k - \mathbf{v}_i\|/\|\mathbf{x}_k - \mathbf{v}_j\|)^{\frac{2}{m-1}}\;\Big]^{-1}, \; \forall\; i,k \; . \qquad (4)$$

And update V again with equation (3).

Step 3: Stop the FCM if $\max_{i\in[1,C]} \|\mathbf{v}_i - \mathbf{v}_i^{(0)}\|_\infty < \epsilon$, where $\epsilon = 0.5$ for sub-level precision and $\|\cdot\|_\infty$ is the L-infinity vector norm (i.e., the maximum of absolute values of the entries in the corresponding vector). Otherwise, $\mathbf{v}_i^{(0)} = \mathbf{v}_i$, return to Step 2.

Step 4: Segment X into $\{H_i\}_{i=1}^C$ by maximum membership de-fuzzification as: $\mathbf{x}_k \in H_i$, if $\max_{j\in[1,C]}(u_{jk}) = u_{ik}$.

The FCM clustering result of Fig. 1(a) is shown in Fig. 1(d); we use it for the segmentation-based locally adaptive weighted median and weighted average filterings in next section.

6. ADAPTIVE ENHANCEMENT AND SEGMENTATION

Conventional linear/nonlinear filters always employ fixed-shape and fixed-size templates in a sliding window to perform convolutions [9]. The pixel to be filtered is generally the center pixel of the window. The entries in filtering templates can be decided in a nonlinear manner by statistics calculated from the current window. Normally the stationarity in the window is assumed. However, this assumption is not always true for MRI images, especially to the edge pixels which are effected by partial volume effects.

Wavelet shrinkage with universal threshold performs a simple and global de-noising which suppresses all the pixels with small detail coefficients. But on the other side, it's based on the assumption of additive white Gaussian noise and not spatial-scale adaptive thus ignores much of the spatial correlation information. Therefore for the signal-dependent noise like Rician noise, universal shrinkage will leave some noises un-suppressed and edges blurred. We can find these limitation from the filtering result in Fig. 1(b) and from the misclassifications in the segmentation result in Fig. 1(d).

Meanwhile, the FCM clustering result gives us some useful information about partial volume effects via the fuzzy membership matrix U. In this context, we proposed a locally adaptive enhancement scheme based on the clustering result which indicates locally a kind of spatial correlationship and stationarity.

Generally a pixel within H_i and farther away from edges has higher membership degree to H_i than the edge pixels. For such a pixel, we suppose that a more stationary neighborhood of its can be constructed using the pixels which were segmented into the same region with it and are in the sliding window with it being the center pixel. This neighborhood, varying in the size and shape, considers both the correlationship in the feature space via a segmentation and in spatial domain via a sliding window. The average filtering is used in such a neighborhood. For the pixels whose maximum membership degrees are not high enough (e.g., less than 75%), we use adaptive median filtering in the whole sliding window to remove noise and avoid destroying details and structures as what average filtering suffers from.

Furthermore, we use maximum membership degrees as weights of the elements within a filtering template. To calculate average and median with the weights of membership degrees will favor the willing of replacing the edge pixels with the center pixel of a segments. It inclines to enhance a structure like edge and to increase the homogeneity within each region, and thus improves the performance of the further FCM clustering.

6.1. Implement of Locally Adaptive Enhancement

First we make several denotations. $u_i(x, y)$ denotes the membership degree of a pixel (x, y) to the i-th cluster; it can be obtained from the matrix U in the previous FCM, if we arrange each pixel as an individual data sample in X. $H_{(x,y)}$ denotes the cluster that (x, y) was classified into after the de-fuzzification in the FCM, and $u_{(x,y)} = \max_{i\in[1,C]}(u_i(x, y))$. $SW_{(x_0,y_0)} = \{(x, y) \mid x \in [x_0-2, x_0+2], y \in [y_0-2, y_0+2]\}$ is a 5×5 sliding window with its center pixel (x_0, y_0). $f(x, y)$ is the intensity of (x, y).

Then the implement of the FCM-weighted adaptive median filtering on this pixel (x_0, y_0) is as follows.

Step 1: If $u_{(x_0,y_0)} < u_{th}$, we update $f(x_0, y_0)$ using a weighted median filtering in $SW_{(x_0,y_0)}$. $u_{th} \in [0, 1]$, which in our case 75%, is a parameter to measure the reliability and validity of FCM clustering result. Firstly we sort the intensities of all the pixels within $SW_{(x_0,y_0)}$ in ascending order, denoting the sorted intensities as $(f_1, f_2, \cdots, f_{25})$ and corresponding maximum fuzzy membership degrees as $(u_1, u_2, \cdots, u_{25})$. Subsequently, the median f_m is decided by

$$m = \min\{i \mid \sum_{j=1}^{i} u_i \geq \bar{u}\}\,, \tag{5}$$

where $\bar{u} = \sum_{i=1}^{25} u_i/2$. As you can find, the weight of each pixel is the corresponding fuzzy membership degree. In such a way, the updated $f(x_0, y_0) = f_m$ is in favor of the intensity with highest degree in its neighborhood, and the misclassifications of those pixels with similar degrees to two brain tissues will be reduced. Go to Step 3.

Step 2: Construct a neighborhood set $\Omega_{(x_0,y_0)}$ as

$$\Omega_{(x_0,y_0)} = \{(x, y) | H_{(x,y)} = H_{(x_0,y_0)}, (x, y) \in SW_{(x_0,y_0)}\}, \tag{6}$$

then replace the intensity of (x_0, y_0) with a weighted average over pixels in $\Omega_{(x_0,y_0)}$ as

$$f(x_0, y_0) = \sum_{(x,y)\in\Omega_{(x_0,y_0)}} u_{(x,y)} f(x, y) \;/ \sum_{(x,y)\in\Omega_{(x_0,y_0)}} u_{(x,y)}\,. \tag{7}$$

Similarly, the average is also affected more by the pixel with higher degree, normally the pixel closer to the prototype of same cluster to which (x_0, y_0) belongs. In such a way, the homogeneity within each cluster is improved.

Step 3: Move the sliding window to the next position, return back to Step 1 unless every pixel in the image has already been processed once as a center pixel.

6.2. Segmentation after Adaptive Enhancement

The FCM will be applied once more to segment the image which has been filtered by the aforementioned adaptive median filtering. The median filtering and segmentation results of Fig. 1(a) can be found respectively in Fig. 1(e) and Fig. 1(f). After comparing the Fig. 1(d) and Fig. 1(f), we can find in the latter the refinement of noise removal and edge preservation. To be noted is that the performance of such an adaptive median filtering depends on the accuracy of a preceding segmentation. Hence using an iteration of filterings and segmentations can improve the accuracy of the final segmentation. But the price of this iteration is the computation complexity and the risk of giving rise to unwarranted enhancement on edges between different segments. From our experiments, we found that more iterations have given little improvement on the validations of segmentation results.

7. QUANTITATIVE VALIDATION AND CONCLUSION

To quantitatively validate our method, testing images with the "ground truth" are required. A realistic digital brain phantom was proposed in [6] considering the partial volume effects. A discrete anatomical model of three brain tissues is derived from the phantom by assign the pixel a label of the tissue which contributes the most to that pixel. This model serves as the "ground truth" in our quantitative validation. Based on this phantom, four realistic MRI images are simulated with T1-weighted sequences, slice thickness of $1mm$, intensity inhomogeneities of 40%, and noise levels of 3%, 5%, 7% and 9% respectively. The brain of interest is firstly extracted with the guidance of the "ground truth", then segmented by our proposed method.

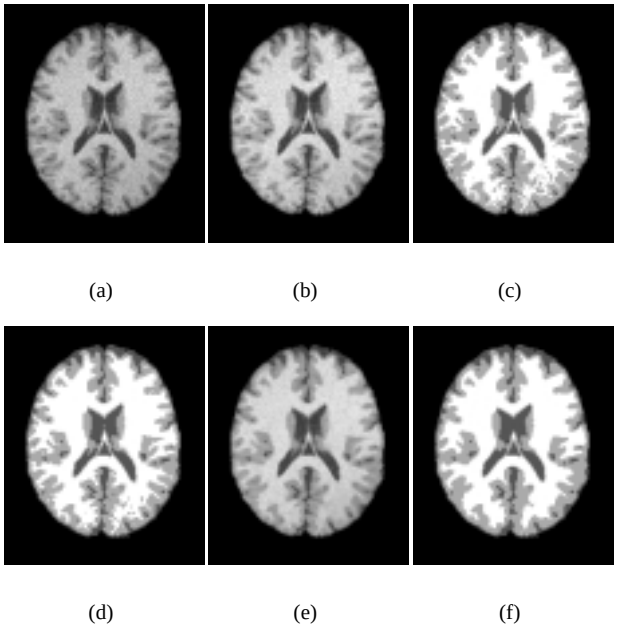

(a) (b) (c)

(d) (e) (f)

Fig. 1. (a) Original image from MRI brain phantom with 9% noise level and 40% intensity inhomogeneities, and its processed versions with (b) wavelet-based de-noising; (c) minimum error thresholding; (d) FCM clustering; (e) adaptive median filtering; (f) final segmentation result.

We employ four different indices (false positive ratio γ_{fp}, false negative ratio γ_{fn}, similarity index ρ [10], and Kappa statistic κ [10]) for each of three brain tissues as quantitative measures to validate the accuracy and reliability of our method. $\rho, \kappa > 0.7$ indicates a well acceptable result [10]. The quantitative validation results of aforementioned four images are plotted in Fig. 2. γ_{fp} and γ_{fn} of GM are approximately 15% and 12% respectively, both larger than those of CSF and WM. Meanwhile, ρ and κ of GM are around 86% and 78% respectively, both less than those of CSF and WM. For anyone of the three brain tissues, the maximum difference between two noise levels is less than 2% in γ_{fp}, γ_{fn} and κ, and less than 1% in ρ. Particularly between the noise levels of 3% and 5%, the differences in all the four indices are quite small. From the Fig. 2, we can also find that: with the noise level increasing, γ_{fp} and γ_{fn} are approximately monotonically increasing, while ρ and κ are approximately monotonically decreasing.

Up to now, we have presented and validated a global-to-local method for the adaptive enhancement and unsupervised segmentation of three brain tissues (CSF, GM and WM) in MRI brain images. This method endows the segmentation with an encouraging performance even in noisy images. Although this method is only with 2-D implementation, the extension to 3-D volume segmentation is currently being investigated.

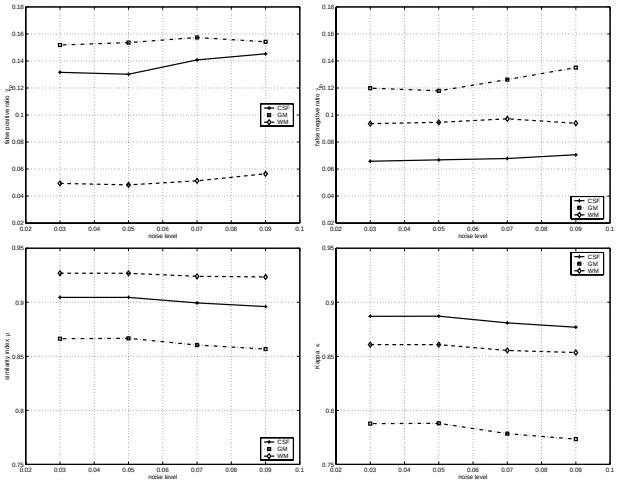

Fig. 2. From top to bottom: validation results for different noise levels with measures of (a) false positive ratio γ_{fp}; (b) false negative ratio γ_{fn}; (c) similarity index ρ; (d) Kappa statistic κ.

8. REFERENCES

[1] L.P. Clarke et al., "MRI segmentation: methods and application," *Magnetic Resonance Imaging*, vol. 13, no. 3, pp. 343–368, 1995.

[2] W.J. Niessen et al., "Multiscale segmentation of three-dimensional MR brain images," *International Journal of Computer Vision*, vol. 31, no. 2/3, pp. 185–202, 1999.

[3] D.L. Donoho and I.M. Johnstone, "Ideal spatial adaption by wavelet shrinkage," *Biometrika*, vol. 81, no. 3, pp. 425–455, 1994.

[4] S.G. Mallat, *A Wavelet Tour of Signal Processing*, Academic Press, San Diego, 2nd edition, 1999.

[5] H. Gudbjartsson and S. Patz, "The Rician distribution of noisy MRI data," *Magnetic Resonance in Medicine*, vol. 34, no. 6, pp. 910–914, 1995.

[6] D.L. Collins et al., "Design and construction of a realistic digital brain phantom," *IEEE Trans. Medical Imaging*, vol. 17, no. 3, pp. 463–468, 1998.

[7] J. Kittler and J. Illingworth, "Minimum error thresholding," *Pattern Recognition*, vol. 19, no. 1, pp. 41–47, 1986.

[8] J.C. Bezdek, *Pattern Recognition with Fuzzy Objective Function Algorithms*, Plenum Press, New York, 1981.

[9] J. Astola and P. Kuosmanen, *Fundamentals of Nonlinear Digital Filtering*, CRC Press, Boca Raton, 1997.

[10] A.P. Zijdenbos et al., "Morphometric analysis of white matter lesions in MR images: method and validation," *IEEE Trans. Medical Imaging*, vol. 13, no. 4, pp. 716–724, 1994.